

# Remaining Capacity Evaluation of Corroded Belt Conveyor Support Structure

Kazumasa HISAZUMI\* Ryoichi KANNO  
Tomonori TOMINAGA Yoshiaki SHIA

## Abstract

*In recent years, accidents and damage to aging structures have been reported. Sudden collapse has frequently occurred in typical industrial steel structures such as belt conveyor frames. It becomes more important to evaluate residual strengths of the structures in a quantitative manner. Nippon Steel & Sumitomo Metal Corporation has developed a method to evaluate remaining capacity of corroded belt conveyor support structure. In this paper, an extensive compressive test and numerical analysis of corroded channel and angle steel members obtained from real structures are conducted. An axial compressive strength formula of the corroded members and a method to estimate life expectancy of facility are proposed based on the experimental and numerical studies.*

## 1. Introduction

In recent years, accidents and the damage to aging structures which were built during the past rapid economic growth era have been reported, and the equipment maintenance and control technologies that contribute to the national resilience have become of paramount importance. Therefore, close cooperation in research and development among the industrial, government and academic spheres is strongly required. For example, as many of the steel belt conveyor support structures as shown in Fig. 1 are exposed to the external environment, equipment problems considered to be caused by the structural deterioration due to corrosion have occurred in Nippon Steel & Sumitomo Metal Corporation. These problems are mainly due to the facts that the steelworks are located in coastal areas, that dust accumulated on the structures during operation of the facilities makes it difficult to check the corrosion condition, and further that many of these structures are truss-type structures with less redundancy. The occurrences of accidents due to the aging of the equipment not only influences the business directly by the plant operation shutdown and restoration work, but has also exposed the serious risks involved in securing safety and establishing social trust. To cope with such risks, countermeasures such as renewal, repairing and reinforcing have already been applied sequentially in the order of the seriousness of the risk of the respective equipment. On the other hand, even after the countermeasures are taken, as the degra-

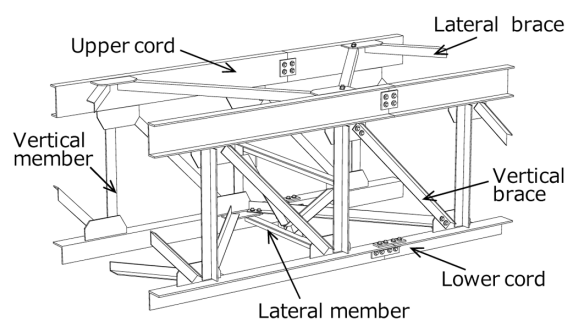


Fig. 1 Typical belt conveyor support structure

ation over time will progress due to corrosion depending on the state of coating, it is necessary to estimate the future risk accurately and implement maintenance control appropriately to prevent the outbreaks of contingent accidents. Accordingly, the development of the technology that can evaluate the soundness of structures quantitatively taking into account the state of the degradation over time has become an urgent issue.

This report describes the efforts made to establish the soundness evaluation technologies of corrosion-deteriorated steel structures and their applications in future.

\* Researcher, Steel Structures Research Lab., Steel Research Laboratories  
20-1 Shintomi, Futtsu City, Chiba Pref. 293-8511

## 2. Diagnosis Technologies of Steel Structural Equipment and Problems

The soundness evaluation of general steel structures is conducted through visual inspection of the extent of corrosion-deterioration and by comparing the result with the prepared evaluation standard such as with sample photographs. The extent of deterioration in each member is evaluated and the repair work is conducted in the order of equipment priority. On the other hand, this method, although convenient, is strongly influenced by subjective and qualitative factors. As the entire evaluation is based only on the evaluation of each member, this method is unable to evaluate directly the remaining strength of the entire equipment (entire structural system) that consists of plural members. Specifically, the relationship between the extent of deterioration of each member and the remaining strength of the entire equipment as a whole unit is unclear. Therefore, the quantitative indices that determine the timing of repair and/or renewal of the equipment, and the priorities thereof are currently unavailable. Accordingly, there are stronger requests for an objective and quantitative evaluation method from the field maintenance staff that aims for the formulation of the most optimized maintenance control plan, and therefore, technologies that are capable of evaluating the soundness of the entire equipment.

Under such circumstances, a belt conveyor support structure was used as a representative steel structure, and the evaluation method of the remaining strength of the steel member that has changed its shape complicatedly due to corrosion was established. Furthermore, the technology to evaluate the remaining capacity of the entire structural system considering its member strength has been developed.

## 3. Behavior of Corroded Steel Member under Axial Compression

As the belt conveyor support structure basically has a truss-structure, the study on the remaining strength needs to be conducted subject to the axial force such as tension and compression that acts predominantly as the sectional force. On the other hand, there are many researches on the tension applied to naturally-corroded channel members and angle members that are generally used in industrial steel structures. However, researches conducted on the buckling behavior under compression are rare globally. Therefore, the evaluation method of the compression strength that is sensitive to the corroded shape and the state of corrosion has not yet been sufficiently established. Thus, samples of the members with light corrosion and the members with severe corrosion such as remarkable sectional area loss due to pitting were taken from a belt conveyor support structure that had been in service for many years. The buckling behavior was analyzed in detail with axial compression tests and FEM analysis.

### 3.1 Characteristics of corroded steel members

A total of 27 corroded test specimens (10 channels and 17 angles) had rust removed by sand blasting and their surface profiles were measured precisely at intervals of 1 mm in the vertical and horizontal directions using a 3D laser displacement sensor (REVscan™). The measured geometric data gives not only the residual thickness, but also the geometric information of the local deformation along the member axis direction caused by the corrosion and the initial curvature that existed before corrosion. **Figure 2** shows an example of cross sectional area distribution along the axis of a member. The sectional area varies significantly in the height direction due to the influence of corrosion.

**Table 1** gives the specimen data including type of shape, length

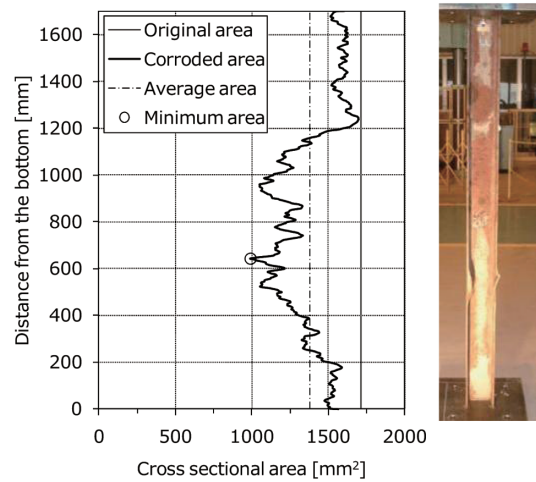


**Fig. 2** Example of cross sectional area distribution along member axis

$L$ , yield strength  $\sigma_y$ , sectional dimensional elements of original members before corrosion (sectional dimension, cross-sectional area  $A_0$ , largest width-thickness ratio parameter of the plate element of the section  $\lambda_{p0}$ ), and the sectional dimensional elements of the corroded members (minimum cross-sectional area  $A_{\min}$ , average cross-sectional area  $A_{\text{ave}}$ , maximum corrosion ratio  $R_{\max}$ , average corrosion ratio  $R_{\text{ave}}$ , size of pit). In the table, the corrosion ratio is defined as the ratio of the cross sectional area reduced by sectional area loss due to corrosion vs. the sectional area before corrosion  $A_0$  and defined by the formulae below.

$$R_{\max} = \frac{A_0 - A_{\min}}{A_0} \times 100 \quad (1a)$$

$$R_{\text{ave}} = \frac{A_0 - A_{\text{ave}}}{A_0} \times 100 \quad (1b)$$

The corrosion ratios defined by formula (1a) and formula (1b) are zero % for the specimens without corrosion and are 100% for specimens wherein the sections have been completely corroded. In the target specimens, the maximum corrosion ratio  $R_{\max}$  ranges from 8% to 74%, the average corrosion ratio  $R_{\text{ave}}$  ranges from 6% to 51%, and the degree of corrosion extends relatively over a wide range.

**Figure 3** shows the relation between the corrosion ratios (average and maximum) and the coefficient of variation (C.O.V) of the cross-sectional area plotted for the respective test specimens. With the increase in either of the maximum corrosion ratio ( $\square$ ) and the average corrosion ratio ( $\blacktriangle$ ), the coefficient of variation for both average and maximum cross sectional area losses tends to increase. This means that as the extent of corrosion increases, the state of corrosion of the member in the axial direction becomes more complex.

### 3.2 Axial compression test of corroded steel members

Each specimen having a base plate welded at each end was subject to an axial compressive test under the boundary condition of both ends being fixed so as to make the buckling length distinct (**Fig. 4**). To minimize the influence of eccentricity, one surface of the base plate was stably machined and grout was poured thinly into the space between another surface of the plate and the loading surface of the test machine and was solidified. Thus, a state of adherence was secured. The loading test was conducted under displacement control and the displacement between the two plates at both ends of the specimen was taken as the basis for measuring the load, with the load being measured at 0.05 mm intervals of displacement. The loading was completed when the buckling deformation became

Table 1 Outline of test specimens

Specimen name	Type of shape	Length [mm]	Yield strength [N/mm <sup>2</sup> ]	Data for original members						Data for corroded members				
				Section size [mm]				Cross-sectional area [mm <sup>2</sup> ]	Largest width-thickness ratio parameter	Cross sectional area [mm <sup>2</sup> ]		Ratio of area loss to original area [%]		Size of pit [mm]
				b <sub>1</sub>	b <sub>2</sub>	t <sub>w</sub>	t <sub>f</sub>			A <sub>0</sub>	λ <sub>p0</sub>	A <sub>min</sub>	A <sub>ave</sub>	
								Minimum	Average					Maximum
C-1	Channel	1700	307	125	65	6	8	1711	0.51	876	1207	49	29	17×56
C-2	Channel	1700	307	125	65	6	8	1711	0.51	970	1286	43	25	19×23
C-3	Channel	1700	307	125	65	6	8	1711	0.51	991	1382	42	19	8×6
C-4	Channel	1700	307	125	65	6	8	1711	0.51	845	1423	51	17	7×8
C-5	Channel	1700	307	125	65	6	8	1711	0.51	861	1315	50	23	11×18
C-6	Channel	1700	307	125	65	6	8	1711	0.51	452	844	74	51	418×95
C-7	Channel	1700	307	125	65	6	8	1711	0.51	1014	1364	41	20	32×11
C-8	Channel	1700	307	125	65	6	8	1711	0.51	872	1194	49	30	31×31
C-9	Channel	1700	307	125	65	6	8	1711	0.51	903	1366	47	20	12×27
C-10	Channel	1700	307	125	65	6	8	1711	0.51	468	1127	73	34	95×76
L-1	Angle	800	325	50	50	-	4	389	0.80	167	237	57	39	32×8
L-2	Angle	800	325	50	50	-	4	389	0.80	187	269	52	31	435×11
L-3	Angle	800	304	50	50	-	6	564	0.52	489	507	13	10	No pit
L-4	Angle	800	304	50	50	-	6	564	0.52	496	514	12	9	No pit
L-5	Angle	800	304	50	50	-	6	564	0.52	231	427	59	24	No pit
L-6	Angle	250	304	50	50	-	6	564	0.52	166	298	71	47	38×43
L-7	Angle	1000	304	50	50	-	6	564	0.52	440	497	22	12	No pit
L-8	Angle	900	338	65	65	-	6	753	0.71	549	628	27	17	No pit
L-9	Angle	500	327	65	65	-	6	753	0.70	662	676	12	10	No pit
L-10	Angle	500	327	65	65	-	6	753	0.70	655	678	13	10	No pit
L-11	Angle	500	311	75	75	-	9	1269	0.52	837	1068	34	16	No pit
L-12	Angle	750	303	75	75	-	9	1269	0.52	1110	1189	13	6	No pit
L-13	Angle	750	303	75	75	-	9	1269	0.52	689	876	46	31	32×16
L-14	Angle	750	303	75	75	-	9	1269	0.52	1134	1168	11	8	No pit
L-15	Angle	750	303	75	75	-	9	1269	0.52	802	941	37	26	No pit
L-16	Angle	750	303	75	75	-	9	1269	0.52	1167	1191	8	6	No pit
L-17	Angle	750	303	75	75	-	9	1269	0.52	722	836	43	34	No pit

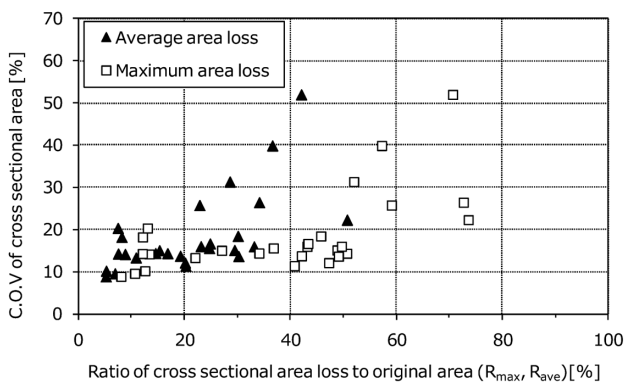


Fig. 3 Relation between corrosion ratio and C.O.V of cross sectional area

visually clear after the maximum load to the specimen was reached. Further, as there were members with remarkable surface unevenness developed by corrosion and members accompanying complicated

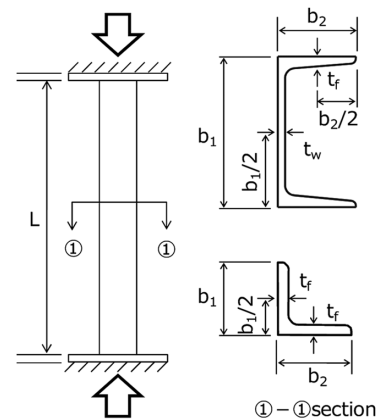


Fig. 4 Compression test schema and definition of specimen size

outer surface deformation, the strain gauges and the displacement gauges for the direction perpendicular to the vertical axis were not installed.

Table 2 Outline of test result

Specimen name	Maximum strength		Observed failure mode	Slenderness ratio parameter
	$P_{max}$ [kN]	$\sigma_{max}/\sigma_y$		
C-1	204	0.71	Local-Global	0.50
C-2	240	0.75	Local-Global	0.53
C-3	278	0.85	Local-Global	0.56
C-4	209	0.75	Local-Global	0.50
C-5	162	0.57	Local-Global	0.47
C-6	47	0.32	–	0.53
C-7	305	0.91	Local-Global	0.49
C-8	172	0.64	Local-Global	0.84
C-9	260	0.87	Local-Global	0.51
C-10	109	0.71	Local-Global	0.51
L-1	31	0.56	Local-Global	0.46
L-2	17	0.27	–	0.45
L-3	150	0.96	Yield-Global	0.51
L-4	152	0.97	Global	0.51
L-5	81	1.11	Yield-Global	0.50
L-6	31	0.59	Local-Global	0.15
L-7	155	1.17	Yield-Global	0.64
L-8	191	1.03	Global	0.45
L-9	222	0.99	Global	0.25
L-10	231	1.04	Yield-Global	0.25
L-11	297	1.30	Yield-Global	0.20
L-12	368	1.21	Yield-Global	0.31
L-13	186	0.99	Local-Global	0.41
L-14	423	1.37	Yield-Global	0.32
L-15	237	1.08	Local-Global	0.37
L-16	402	1.26	Yield-Global	0.32
L-17	210	1.06	Local-Global	0.32

Table 2 summarizes the experimental results.  $P_{max}$  in the table represents the maximum strength (maximum load) obtained in the tests.  $\sigma_{max}$  is the maximum strength expressed in terms of stress intensity obtained by dividing  $P_{max}$  by the minimum cross sectional area  $A_{min}$  of the member ( $= P_{max}/A_{min}$ ). Non-dimensional maximum strength normalized by yield strength,  $\sigma_{max}/\sigma_y$ , is distributed relatively widely, from 0.27 to 1.37. The test specimens with  $\sigma_{max}/\sigma_y$  exceeding about 1.0 are accompanied by the sectional yielding.

Based on the visually observed state of the deformation after the maximum strength is reached and the judgement as to whether the sectional plastic deformation exists or not based on  $\sigma_{max}/\sigma_y \approx 1$  as the judging criteria, the ultimate failure mode of the test specimens was categorized into the following four modes as shown in Table 2. These are: 1) the global buckling mode developed after sectional yielding (Yield-Global); 2) the global buckling mode developed before sectional yielding (Global); 3) the global buckling mode coupled to local buckling (Local-Global); and 4) the buckling mode with the local buckling only (Local). Figure 5 shows examples of these ultimate failure modes and the relationship between the load and the displacement. There were two types of global buckling: one is accompanied by torsional deformation and the other is dominated by flexure. However, whether the observed torsional deformation is the result of the flexural torsional buckling or the result of the flexural deformation by the rotation of the main axis around the axis of the member due to local corrosion was not clear from the test results, and they are both handled as global buckling.

Figure 6 shows the relationships between the maximum strength  $P_{max}$  and the average cross sectional area  $A_{ave}$ , and the minimum cross sectional area. Although there is little correlation between the maximum strength and the average cross sectional area (correlation coefficient 0.72), there is a distinctive relationship between the maximum strength and the minimum sectional area with high correlation (correlation coefficient 0.94). This trend is observed in the corroded member that is subject to a tensile force. However, even in the

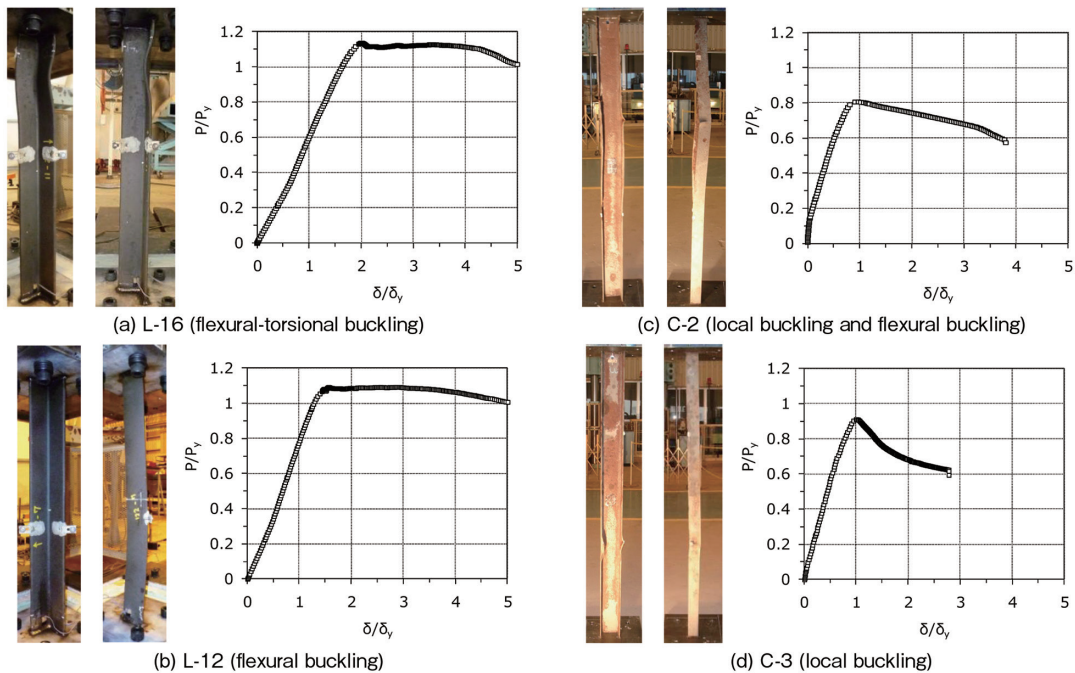


Fig. 5 Examples of photos after loading tests and load-displacement curve

member subject to compression, that the maximum strength is similarly governed by the state of the corrosion at its weakest part (minimum cross sectional area) is a significant finding.

**3.3 FEM analysis taking into 3D geometry of corroded members**

The results of the axial compression tests of the corroded members indicate the existence of a plurality of failure modes and a certain relationship between the minimum cross sectional area and the maximum strength. However, the behavior before reaching the maximum strength, the mechanism that determines the maximum strength in particular, has not been sufficiently analyzed. Therefore, an FEM model taking into account the geometric information obtained through the 3D measurement was developed and the behavior of the corroded member before reaching the maximum strength was studied with special attention focused on the buckling mode that governs the maximum strength.

As the test specimens used in this study are severely corroded and pitting corrosion has developed, it is necessary to reproduce the pitting corrosion that influences the local deformation and/or the strength in the thinned thickness region. Therefore, as a result of several trial studies, considering the minimum pit size of 6 mm confirmed in the test specimens and the balance with the volume of computation, a shell element 2 mm×2 mm was selected for modeling. The plate thickness measured in the respective plate element was averaged and given as a constant value to the thickness of the plate element. Furthermore, to consider the influence of the local yielding developed around the pit by strain concentration, the true stress-true strain relation based on a tensile test was applied. Figure 7 shows schematically the FEM modeling of a member with thick-

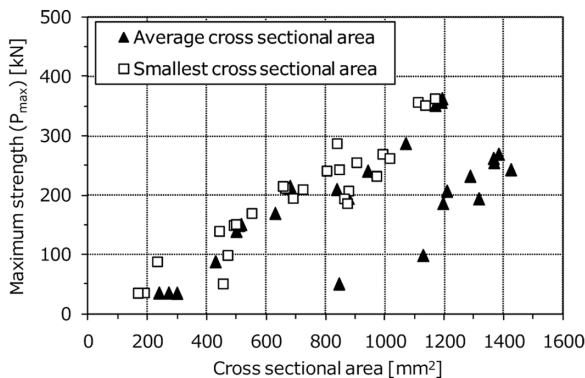


Fig. 6 Relationship between maximum strength and cross sectional area

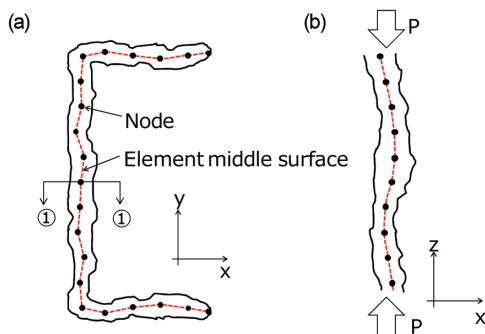


Fig. 7 Outline of FEM modeling (a) Cross section along member axis, (b) ①-① section

ness thinned by corrosion.

Herein, for all test specimens, two types of analysis were conducted. The first type of analysis is to reproduce the tests wherein the conditions that are the same as those of the aforementioned tests are taken into consideration. The second case analysis is for judging the buckling mode, wherein the lateral displacement of the member was restrained in addition to the first case to prevent the occurrence of the global buckling. If the maximum strength in the second case sufficiently exceeds the strength of the first case, the global buckling is meant to dominate the strength. When the maximum strengths in the first case and the second case do not differ greatly, the local buckling or yielding is meant to dominate the strength. Figure 8 shows the restraining condition introduced for the second case. To prevent the influence over the occurrence of the local buckling, the lateral displacement was restrained at the joining point of the plate elements at intervals of three times the minimum width of the plate element.

**3.4 Comparison of test result and analytical result and buckling mode**

Figure 9 shows the plotting of the relationship between the test results and the analytical results. Almost all analytical results lie within a 15% error (shown by broken lines in Fig. 9) and it is judged that the FEM analysis reproduces the test results favorably when the complexity of the state of the corrosion of the subject member is considered. Furthermore, although the residual stress is not taken into consideration in the FEM analysis, the extent of its influence may vary depending on the slenderness ratio. As information regarding the distribution and the magnitude of the residual stress of

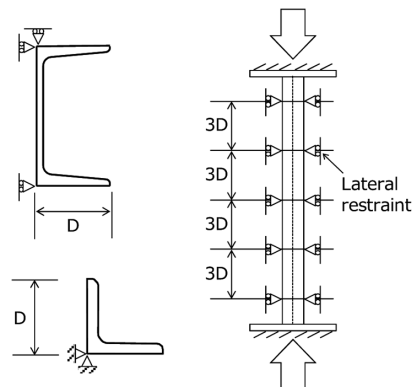


Fig. 8 Boundary condition in case that global buckling is restrained

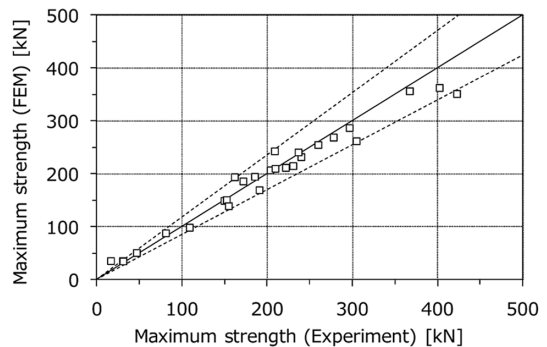


Fig. 9 Comparison of maximum strength of experiment and FEM analysis

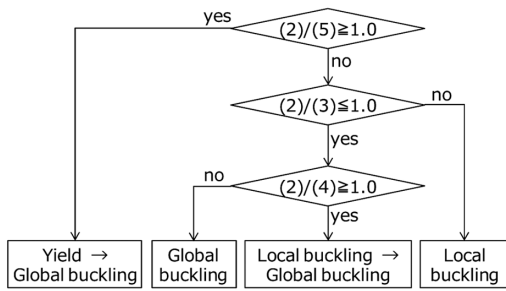


Fig. 10 Judgment for buckling mode

the corroded member is unknown, the residual stress and the influence it has on the buckling behavior are subjects for future study. Further, the test specimens of L-2 and C-6 exhibited fracture in the longitudinal direction at the corner position of an angle steel and a channel steel, and behavior wherein the constituent plates of the members were separated in a manner quite different from buckling. Therefore, the test specimens were not studied in the analysis that follows.

Further, at any of the nodes in the analysis model, when the ratio of  $\Delta\varepsilon$ , the difference between the strain on the front side and that on the rear side of a plate element vs. the average of the said strains  $\varepsilon_{ave}$  is one or above ( $\Delta\varepsilon/\varepsilon_{ave} \geq 1$ ), the load was defined as the local buckling load. Figure 10 shows the flow of judgement for the buckling mode. Firstly, when the maximum strength as a result of the analysis for the case without restraint exceeds the yielding load, the mode was judged as the “sectional yielding mode (Yield-Global)”. Secondly, among the cases wherein the ratios of the maximum strengths without the displacement restraint vs. those with restraint are below 1, the case of the maximum strength exceeding the local buckling load was judged as the “coupled buckling mode to global buckling and local buckling (Local-Global)”. The rest was judged as the “global buckling mode (Global)”. Cases not applicable to any of the above were judged as local buckling mode (Local). As a result of the analysis, there are 8 cases of the sectional yielding mode (Yield-Global), 3 cases of the global buckling mode (Global) and 14 cases of the coupled buckling mode (Local-Global). No cases of local buckling mode (Local) governing the mode were found. The features of the respective mode are outlined hereunder.

The maximum corrosion ratio of the sectional yielding mode is in the range between 11%–22% except those of abnormal test specimens in part, and the extent of the corrosion is moderate. The test specimens of this mode have relatively healthy plate elements. Therefore, the local buckling and/or the local deformation are suppressed, and are characterized by the plasticity developed by the sectional yielding. This mode exhibits no local buckling before reaching the maximum load. After reaching the maximum load, the sectional yielding is developed, and simultaneously the global buckling (flexural buckling) takes place. Afterwards, decrease in load is observed.

The maximum corrosion ratios of the test specimens that exhibit only global buckling mode are in the range between 12%–27%. Before reaching the maximum load, local buckling does not occur, and the displacement in the axial direction increases linearly along with the increase in the load. After the maximum load, the load decreases gradually due to the global buckling.

The maximum corrosion ratios of the test specimens of the mode of the global buckling after local buckling are the highest among the three modes and are in the range between 37%–73%. As the load in-

creases, a local buckling occurred at the left flange where the maximum corrosion ratio existed, and then local buckling occurred at the right flange and the web. On the other hand, in this mode, the local buckling that occurred at the respective plate elements is not the direct determining factor of the maximum load (maximum strength), and ultimately the maximum strength was determined by the global buckling (flexural buckling). This is considered to be attributed to, similarly to the case of a member consisting of a thin sheet steel, the stress of a part that has become unbearable locally due to yielding being redistributed to another relatively sound part of the identical cross section.

### 3.5 Proposal of strength evaluation formula for corroded members

The analysis of the buckling modes revealed that the coupled buckling mode of the global buckling and local buckling (Local-Global) is the most frequently observed. Hereafter, the study on the strength evaluation is conducted based on Johnson's parabola formula known as the strength evaluation formula for global buckling, from the viewpoints of to what extent the strength evaluation is possible, and with what means of correction the evaluation accuracy can be improved. As the cross section of the corroded member varies in the axial direction of the member, the selection of the optimum cross-sectional property remains as a problem. In this study, the cross-sectional property of the minimum sectional area that exhibits a high correlation with maximum strength as shown in Fig. 6 is used and the strength of the corroded member is evaluated by the following formula.

$$P_{cr} = A_{min} \cdot \sigma_{cr} \tag{2a}$$

$$\sigma_{cr} = \begin{cases} (1 - 0.24\lambda_n^2) \cdot \sigma_y & (\lambda_n < 1.3) \\ \frac{1}{\lambda_n^2} \cdot \sigma_y & (\lambda_n \geq 1.3) \end{cases} \tag{2b}$$

where  $P_{cr}$ : Global buckling strength (N),  $A_{min}$ : Minimum cross-sectional area (mm<sup>2</sup>),  $\sigma_{cr}$ : Global buckling stress (N/mm<sup>2</sup>), and  $\lambda_n$  is the slenderness ratio parameter that is defined by the following formula considering the correlation with the minimum sectional area observed in Fig. 6.

$$\lambda_n = \frac{1}{\pi} \sqrt{\frac{\sigma_y}{E}} \frac{L_k}{i_m} \tag{2c}$$

where  $\sigma_y$ : Yielding stress (N/mm<sup>2</sup>),  $E$ : Young's modulus (N/mm<sup>2</sup>),  $L_k$ : Effective buckling length (mm),  $i_m$ : Radius of gyration of area around the weak axis at the minimum cross-sectional area (mm).  $i_m$  is determined by the minimum cross-sectional area  $A_{min}$  and the moment of inertia of the area around the weak axis  $I_{min}$ .

$$i_m = \sqrt{\frac{I_{min}}{A_{min}}} \tag{2d}$$

Figure 11 shows the relationship between  $P_{max}/P_{cr}$ , the ratio of the test result vs. the strength calculated by formula (2a), and the maximum corrosion ratio  $R_{max}$ . As the rise in strength in the plastic buckling region is not considered in the evaluation formula applied with Johnson's parabola formula, when the maximum corrosion ratio is 40% or less, it may be possible to evaluate the test result strength  $P_{max}$  on the safe side ( $P_{max}/P_{cr} > 1$ ). On the other hand, when the maximum corrosion ratio is higher than 40%, the evaluation accuracy deteriorates rapidly and the evaluation moves onto the unsafe side. This is because the occurrence of the local buckling becomes remarkable as the maximum corrosion ratio increases and exceeds the applicable range of Johnson's parabola formula.

As shown in Fig. 11,  $P_{max}/P_{cr}$  on the vertical axis gradually decreases as the maximum corrosion ratio increases. Therefore, a cor-

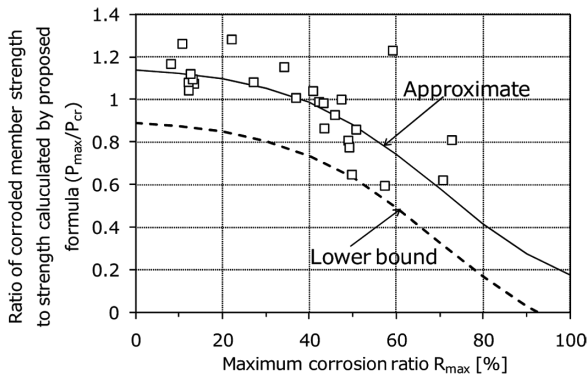


Fig. 11 Relationship between  $P_{max}/P_{cr}$  and  $R_{max}$

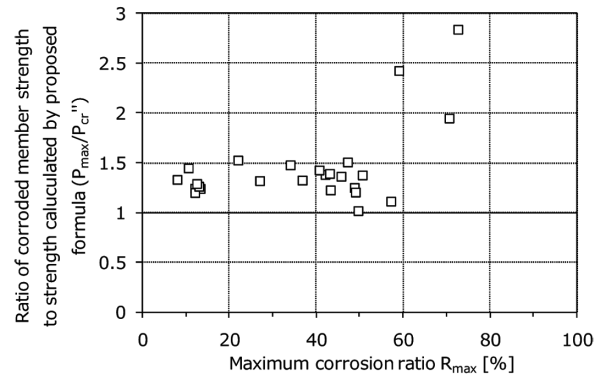


Fig. 12 Relationship between  $P_{max}/P_{cr}''$  and  $R_{max}$

rection factor  $\alpha$  is proposed by taking the maximum corrosion ratio  $R_{max}$  as a parameter. For the evaluation of  $\alpha$ , a formula used for expressing the transition temperature curve of the fracture toughness of a steel has been applied.

$$P_{cr}' = \alpha \cdot P_{cr} = \alpha \cdot A_{min} \cdot \sigma_{cr} \quad (3a)$$

$$\alpha = \frac{6.6}{\exp\{0.058(R_{max} - 40)\} + 5.7} \quad (3b)$$

where  $\alpha$  is the approximation of  $P_{max}/P_{cr}'$  obtained by the minimum square method using a transition temperature curve, and  $R_{max}$  is the maximum corrosion ratio (%). The full line in Fig. 11 is the approximation (3b), which is generally in agreement with the trend of the plotted results. As Formula (3b) is proposed based on the minimum square method, it tends to provide the evaluation on the unsafe side considerably. Therefore, the following formula wherein  $\alpha$  is modified to a minor degree in view of the practicability in the actual use is proposed.

$$P_{cr}'' = \alpha' \cdot P_{cr} = \alpha' \cdot A_{min} \cdot \sigma_{cr} \quad (4a)$$

$$\alpha' = \frac{6.6}{\exp\{0.058(R_{max} - 40)\} + 5.7} - 0.25 \quad (4b)$$

Figure 12 shows the relationship between  $P_{max}/P_{cr}''$  obtained by the above Formulae and  $R_{max}$ . The proposed Formula (4a) enables appropriate evaluation of the test data near the lower bound and can be utilized as a strength-evaluation formula on the safety side.

On the other hand, the abovementioned strength-evaluation formula requires the radius of the gyration of area  $i_m$  of the minimum sectional area based on its cross-sectional property. However, the calculation of the moment of inertia of minimum area  $I_{min}$  is troublesome because of its complicated sectional geometric configuration. Herein, Fig. 13 shows the relationship between  $i_m/i$ , the ratio of radius gyration of the minimum area to that of the original area, and the maximum corrosion ratio  $R_{max}$ . When the maximum corrosion ratio exceeds about 40%, several values of  $i_m/i$  are below 1. However, when the maximum corrosion ratio is about 40% or less,  $i$  is considered to be applicable, substituting  $i_m$ . Therefore, although there are cases wherein the excessively safe evaluation is provided in part, the following Formula ( $P_{cra}$ ) wherein the global buckling stress  $\sigma_{cr0}$  of the original member before corrosion is applied instead of  $\sigma_{cr}$  of Formula (4a) realizes the estimation of the maximum strength with practically sufficient accuracy.

$$P_{cra} = \alpha' \cdot A_{min} \cdot \sigma_{cr0} \quad (5)$$

As the global buckling stress  $\sigma_{cr0}$  of the sound member is already known as the design information of a structure, if the minimum sectional area  $A_{min}$  of the corroded member only is known, the maxi-

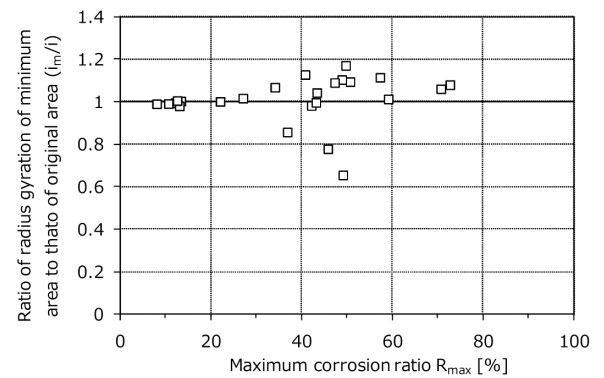


Fig. 13 Relationship between  $i_m/i$  and  $R_{max}$

imum strength can be conveniently estimated. Further, as the proposed Formula (5) is an evaluation formula developed solely based on this test result, the expansion of its application range and the improvement in accuracy by accumulating data are subjects for future study.

## 4. Evaluation of Remaining Capacity of Belt Conveyor Support Structure and Soundness

### 4.1 Concept of modeling

The remaining capacity of the entire structural system needs to be evaluated as the influence of the corroded member on the remaining capacity varies greatly depending on its location even if the extent of the deterioration is the same. The damaged belt conveyor support structure withstands the long-term load (vertical load such as dead load) under operation. Therefore, to evaluate the remaining capacity, the evaluation of the resistance force against the short-term load (horizontal load such as wind load and/or earthquake load) is important. Then, aiming at an evaluation method of high versatility that realizes practicability in actual use, a frame model used in the general design is used in this study. Figure 14 shows the outline of the model. The entire structure is modeled wherein all members constitute beam elements. As for the joint of the member ends, the main members such as the upper chords and the lower chords are considered to be continuous (rigid-joint) and the secondary members such as the diagonal members and the strut members are considered to be pin-jointed. Using the section modulus determined based on the actually measured data, the analysis is then conducted, considering fracture phenomenon under the tensile stress condition and buckling phenomenon under the compression stress condition

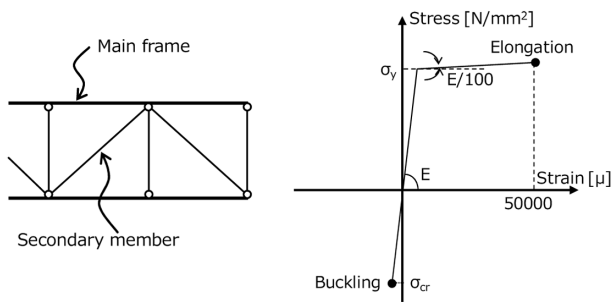


Fig. 14 Modeling scheme and backbone curve for steel member

(Fig. 14).

4.2 Analytical method

The object is an entire structural model acted upon by the horizontal load (short-term load) and the remaining strength (the maximum load at the time of collapse of a structure) is evaluated by the push-over analysis. When the tensile strain of a member exceeds the fracture strain (assumed as 5%) (occurrence of fracture), or when the compression stress acting on the member reaches the buckling stress  $\sigma_{cr}$  (occurrence of buckling) during the process of the push-over analysis, the analysis is suspended temporarily and the new state of equilibrium after removing the subject member from the model of the structure is recalculated and the push-over analysis is restarted. By repeating such a process, the collapsing behavior of the entire structure with due consideration paid to the fracture and the buckling of members was later estimated.

4.3 Remaining capacity of entire structural system and critical members

Figure 15 shows the model frame used for analysis. The model 1 exhibits the sound state, the model 2 exhibits the state of the frame model wherein the thickness of all the members on the lower face is thinned by 30%, and the model 3 exhibits the state of the frame model wherein only the members with 30%-thinned thickness at the end portions on the lower face are remaining. The model 2 and the model 3 are introduced based on the result of the on-site study that the members on the lower face of the support structure are suffering from extremely serious corrosion. Figure 16 shows the results of the analysis. As a matter of course, the remaining strength of the sound model 1 is the highest. However, the remaining strength of the model 3 is scarcely different from that of the model 2 despite the members being fewer in number. This result means that the members near the span ends on the lower face determine the remaining strength to withstand the horizontal load. From the results of the analysis of the model 3 shown in Fig. 15 and Fig. 16, the contribution to the remaining strength of the entire structural system of the members on the lower face other than those near the span ends is small.

Although details are not described, from the results of the study conducted on the collapsing loads of entire structures having a plurality of different corrosion patterns, it was recognized that the buckling of the members near the span ends on the lower face or the fracture of the lower chord at its center is the major cause of the collapse. In other words, in the typical belt conveyor support structures, the members near the span ends on the lower face and the center portions of the lower chords become the important members in securing the remaining strength (termed as critical members). From the viewpoint of maintenance control, the effective suppression of the collapse is considered possible by intensive control of such

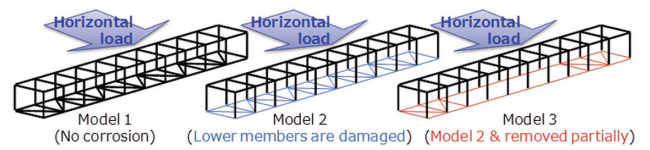


Fig. 15 Frame analysis model

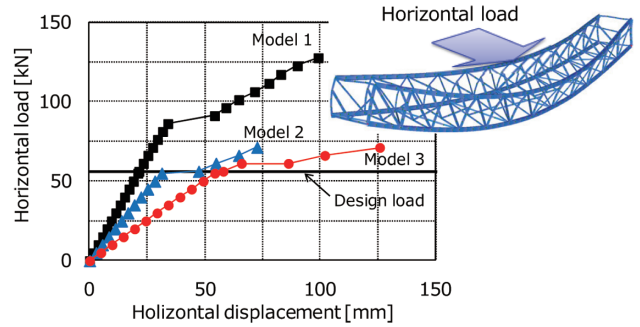


Fig. 16 Horizontal load - displacement curve by frame analysis

members.

4.4 Soundness evaluation of entire structural system

Even if the remaining strength is calculated with the entire structural model, as the horizontal load (short-term load) is the result of natural phenomena and the maximum value constantly varies, the calculated remaining strength does not show the risk of collapsing. Based on the notion that the external forces can be expressed as a probability matter, the quantification of the risk of collapsing is referenced.

The wind load and/or the earthquake load are considered as the horizontal load acting on a structure. As the industrial belt conveyor support structures are installed in elevated locations, the wind receiving areas, and as they are built adjacently to coastal areas where the basic wind velocity is high, the wind load is dominant in designing in many cases. Therefore, the risk of wind is evaluated hereunder.

According to Recommendations for Loads on Buildings, the return period  $T$  (year) of the maximum wind load is expressed by Formula (6).

$$T = \exp\left(\frac{k_{Rw} + 2.9\lambda_U - 3.9}{0.63(\lambda_U - 1)}\right) \tag{6}$$

where  $k_{Rw}$  is the return period conversion factor and is the square root of the value of  $P_u$ , the maximum load obtained by the analysis divided by the design wind load of  $P_d$ , ( $= (P_u/P_d)^{1/2}$ ).  $\lambda_U$  is the factor determined according to the geographical condition of the construction site and is the ratio of  $U_{500}$ , the value corresponding to the return period of 500 years of the average wind velocity of during 10 minutes at the height of 10 m above ground, vs. the basic wind velocity  $U_0$ , ( $= U_{500}/U_0$ ) in the concerned region. As the design wind velocity  $U_d$  to define the design wind load  $P_d$  is determined for the return period of 100 years, the extent of the soundness  $S$  for the fundamental performance required in designing can be expressed by the following formula.

$$S = T/100 \tag{7}$$

According to Formula (7), when the maximum load  $P_u$  is the same as the design wind load  $P_d$ ,  $T$  becomes 100 years ( $T=100$  years), and the soundness  $S$  becomes 1.0 ( $S=1.0$ ). Figure 17 shows the soundness curve obtained from Formula (6) and Formula (7) with the plotted result of the soundness evaluation in the model 3 as an

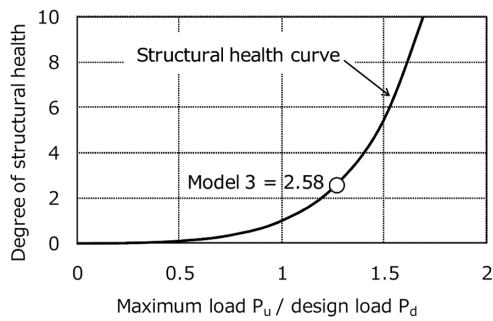


Fig. 17 Relationship between degree of structural health and  $P_u/P_d$

example. When the maximum strength decreases along with the deterioration by corrosion (decrease in the horizontal axis direction), the soundness decreases exponentially (decrease in the vertical axis direction). This means that the risk of collapsing due to decrease in the remaining strength increases more rapidly than the rate of the decrease in the remaining strength. Therefore, it is very important to conduct the monitoring in addition to the periodical diagnosis particularly for the severely corroded members that make a high contribution to the remaining strength of the entire structural system.

In the above, the method of soundness evaluation of the entire belt conveyor support structure system based on the direct investigation of the corrosion is proposed. On the other hand, to grasp the extent of the deterioration correctly, inspectors have to access a plurality of members directly within a limited time and have to measure the remaining thickness of corroded members. Furthermore, when working in an elevated location is required, as the time constraints and the construction of the working platform incur high cost, the first stage evaluation on the grounds of the extent of the deterioration of critical members alone is expected to generate drastic improvement in the working efficiency and lowering of the cost in the deterioration investigation. Hereafter, the improvement for a more practical method, with a view to the application of remote and non-contact deterioration investigation methods through the close tie-up between the equipment control managers and the field workers will become a subject of future study.

## 5. Conclusion

Owing to the soundness evaluation technologies covering the entire structural system as introduced in this report, the continued use of members that are judged as requiring replacement has become possible. Conversely, the severe structural state even with a minor degree of deterioration can be judged in a more quantitative manner. More specifically, the method can clarify the soundness of equipment (risk of collapsing) and the priorities in the maintenance work, and further, is capable of providing information helpful in developing the optimum maintenance plan. We are determined to establish a soundness evaluation technology that is capable of grasping the remaining capacity of the entire structural system based on the element information such as the amount of corrosion and the locations of members in future, furthermore, a systematic technology that contributes to the sophistication of the inspection technology, repair technology and deterioration prediction, and contribute to the solution of various subjects that surround this area of concern.

## References

- 1) Japan Society of Civil Engineers: Manual for Durability Verification of Corroded Steel Structures. 2009.3, p. I-226
- 2) Japan Society of Civil Engineers: Guideline for Stability Design of Steel Structures. 2005.10, p.55-66, 81-104, 149-186
- 3) Architectural Institute of Japan: Recommendations for Stability Design of Steel Structures. 2000.2, p.16-64, 197-230
- 4) Architectural Institute of Japan: Recommendations for Building Loads. 2015, p. 12-20
- 5) The Japan Iron and Steel Federation: Design Manual for Light Gauge Structure. 2008.4, p. 60-95
- 6) Hisazumi, K. et al.: Study on Behavior of Corroded Channel and Angle Members under Axial Compression. 69th Annual Academic Lecture of Japan Society of Civil Engineers, Osaka, 2014, 1-609
- 7) Hisazumi, K. et al.: Axial Compressive Strength of Severely Corroded Channel and Angle Members Used in Truss Structures. EUROSTEEL 2014, Naples, Italy, Vol.A 2014, p. 393-398
- 8) The Japan Welding Engineering Society: Method of Assessing Brittle Fracture in Steel Weldments Subjected to Large Cycle and Dynamic Strain WES 2808. 2003.1, p. 66
- 9) Yamamoto, T. et al.: Shinnittetsu Sumikin Giho. (402), 2-9 (2015)



Kazumasa HISAZUMI  
Researcher  
Steel Structures Research Lab.  
Steel Research Laboratories  
20-1 Shintomi, Futtsu City, Chiba Pref. 293-8511



Tomonori TOMINAGA  
Senior Researcher, Dr. Engineering  
Steel Structures Research Lab.  
Steel Research Laboratories



Ryoichi KANNO  
Fellow, Ph.D.  
R&D Laboratories



Yoshiaki SHIA  
Senior Manager, Head of Dept.  
Mechanical Maintenance Technology Dept.  
Mechanical Engineering Div.  
Plant Engineering and Facility Management Center